NÖHÜ Müh. Bilim. Derg. / NOHU J. Eng. Sci., Erken Görünüm / InPress
Niğde Ömer Halisdemir Üniversitesi Mühendislik Bilimleri Dergisi
Niğde Ömer Halisdemir University Journal of Engineering Sciences
Araştırma makalesi / Research article
www.dergipark.org.tr/tr/pub/ngumuh / www.dergipark.org.tr/en/pub/ngumuh

Investigation of the effect of oxygen flow modulation on ITO film properties to improve the performance of SHJ solar cells

SHJ güneş hücrelerinin performansını artırmak için oksijen akış modülasyonunun ITO film özellikleri üzerine etkisinin araştırılması

Emre Kartal[1,*], Furkan Güçlüer[2], Elif Damgacı[3], Ali Ogün Sarp[4], Ayşe Seyhan[5], Yüksel Kaplan[6]

[1,5] *Niğde Ömer Halisdemir University, Department of Pyhsics, 51240, Niğde, Türkiye*
[1,2,3,4,5] *Niğde Ömer Halisdemir University, Nanotechnology Application and Research Center, 51240, Niğde, Türkiye*
[3,6] *Niğde Ömer Halisdemir University, Department of Mechanical Engineering, 51240, Niğde, Türkiye*

Abstract

Photovoltaic technology offers a sustainable solution for the growing energy needs of the world, while reducing environmental impact. Transparent Conductive Oxides (TCOs), which are essential in photovoltaic technology, offer high light transmittance and effective charge carrier extraction. This research focuses on the impact of oxygen (O_2) flow rates in the deposition of indium tin oxide (ITO) films on n-type crystalline silicon (c-Si) substrates by DC magnetron sputtering. The structural, optical, and electrical properties were analyzed. Based on the results, the optimal O_2 ratio was determined and used in the fabrication of SHJ solar cells, achieving an efficiency of 18.6%.

Keywords: Silicon heterojunction (SHJ) solar cell, DC magnetron sputtering, Transparent conductive oxides (TCOs), Indium tin oxide (ITO)

Öz

Fotovoltaik teknolojisi, dünyanın artan enerji ihtiyaçlarına sürdürülebilir bir çözüm sunarken çevresel etkiyi de azaltmaktadır. Fotovoltaik teknolojide önemli olan şeffaf iletken oksitler (TCO'lar), yüksek ışık geçirgenliği ve etkili yük taşıyıcı ekstraksiyonu sunar. Bu araştırma, DC magnetron püskürtme ile n-tipi kristal silisyum (c-Si) alt tabakalar üzerine indiyum kalay oksit (ITO) filmlerin biriktirilmesinde oksijen (O_2) akış hızlarının etkisine odaklanmaktadır. Yapısal, optik ve elektriksel özellikler analiz edilmiştir. Elde edilen sonuçlara dayanarak, optimum O_2 oranı belirlenmiş ve SHJ güneş pillerinin üretiminde kullanılarak %18,6'lık bir verimlilik elde edilmiştir.

Anahtar kelimeler: Silisyum heteroeklem (SHJ) güneş hücresi, DC magnetron püskürtme, Şeffaf iletken oksitler (TCO'lar), İndiyum kalay oksit (ITO)

1 Introduction

One of the most significant consequences of globalization is the ease of access to products and information. This ease of access has the effect of increasing energy consumption, thereby necessitating an increase in energy demand. As a solution to this energy demand, there has been a notable increase in interest in clean, sustainable, and renewable resources, rather than fossil fuels, compared to previous periods. Particularly, photovoltaic technologies have emerged as effective tools in combating climate change [1-3]. Among various photovoltaic technologies, c-Si-based solar cells stand out due to their advantages such as high energy conversion efficiency, long operational lifespan, cost-effectiveness, and scalability [4,5]. TCOs, are commonly used in solar cells due to their high light transparency, good charge carrier extraction, and overall high performance. The use of TCOs also contributes significantly to better energy conversion efficiency. TCOs are versatile and can be used in a variety of applications such as flexible electronics, flat panel displays, light-emitting diodes (LEDs), fuel cells, dielectric transistors and smartphones [6,7]. ITO is one of the most commonly used TCOs due to its high electrical conductivity. Indium (III) oxide (In_2O_3) and tin (IV) oxide (SnO_2) are combined to form ITO, which is frequently used in a variety of applications, including photovoltaics, as a result of its significant electrical and optical properties [8]. ITO works as an n-type semiconductor material, exhibiting a direct band gap of 3.5 to 4.3 eV [9], a property that enables the fabrication of high-performance materials with superior structural, optical and electrical characteristics [10].

The recent advances in optimizing ITO films are of crucial importance not only for SHJ solar cells but also for thin-film technologies. These advances significantly enhance optical transparency and electrical conductivity, which are vital for the maximization of light absorption and charge collection efficiency. The improvements in ITO films contribute to higher overall performance and stability, making them indispensable for the advancement of both SHJ and thin-film solar cell technologies. The studies demonstrate the value of a comprehensive approach to optimizing ITO films, which requires a detailed understanding of the various properties and fabrication

* Sorumlu yazar / Corresponding author, e-posta / e-mail: emrekartal4271@gmail.com (E. Kartal)
Geliş / Recieved: 29.03.2024 Kabul / Accepted: 27.06.2024 Yayımlanma / Published: xx.xx.20xx
doi: 10.28948/ngmuh.1461409

techniques involved. Some of these studies have resulted in notable advancements, as detailed in Table 1.

Table 1. Optical and electrical effects of ITO films in different studies

Gas Variables	d (nm)	T (%)	R_S (Ω/Sq)	Eg (eV)	Ref.
O_2/O_2 + Ar	48 – 94	93 – 99.6	99.9 – 760.2	3.26 – 3.66	[11]
O_2/Ar	69 – 204	-	270 – $>10^4$	-	[12]
O_2/Ar	80 – 160	85.1 – 89.4	48.71 – 60.99	3.44 – 3.54	[13]
Ar/O_2	91.7 – 191.8	~80 – 90	49 – 332	3.50 – 3.86	[14]
O_2/Ar	252 – 1109	~87 – 92	2.5 – $>400x10^3$	-	[15]
Working Pressure	120 – 170	85 – 90	100 – 10300	3.84 – 3.99	[16]

d (nm): Thickness **T:** Transmission **R_S:** Sheet resistance **Eg:** Band gap

Besides the studies listed in Table 1, this study explored the impact of varying oxygen flow rates during ITO deposition on the performance of silicon heterojunction (SHJ) solar cells. The oxygen flow rates investigated were 0, 1, 1.5, 2, 2.5, and 3 sccm. The resulting ITO films were evaluated for their effects on the power conversion efficiencies (PCE) of the SHJ solar cells produced.

2 Materials and methods

2.1 Thin film deposition

ITO films were deposited onto 1.1 mm thick and 2.5 x 2.5 cm² sized glass substrates using an DC magnetron sputtering system. The sputtering target used was high-purity ITO (99.999%, 5N) [17,18]. The thickness of deposited ITO films was approximately 100 nm. Before introducing the glass substrates into the physical vapor deposition (PVD) chamber, a standard substrate-cleaning procedure was conducted. The process took place at a pressure of $2x10^{-2}$ mbar, 200°C temperature and 2050 W power. To observe effect of the O_2 flow rates to cell efficiency, 0 to 3 sccm (0, 1, 1.5, 2, 2.5, 3) gas flow rate values were used.

2.2 Characterization

Structural properties of ITO films produced at different O2 ratios were analyzed using X-ray diffraction (Pan analytics-XRD J.J with CuKa radiation (λ=0.15406 nm)). The optical properties of ITO films were analyzed using the J. A. Woollam V-Vase Spectroscopic Ellipsometer. In addition, the non-contact layer resistance (EddyCus® TF lab 4040 Hybrid) system was used in electrical measurements of ITO films. The performance of solar cells was analyzed in a clean room at 24°C using the Sinton SunsVoc WCT-120 device on AM-1.5.

2.3 Fabrication of SHJ solar cells

SHJ solar cells were fabricated onto 5x5 cm², random pyramid textured 180 µm thick and (100) oriented c-Si wafers. The c-Si surface was prepared for substrate deposition by removing the oxide layer with an HF solution. The surface was then rinsed with deionized water and dried with nitrogen gas. To passivation of the dangling bonds on the surface of c-Si, 10 nm intrinsic hydrogenated amorphous silicon ((i) a-Si:H) was deposited on both sides of the wafers using the plasma-enhanced chemical vapor deposition (PECVD). The passivation process involved only a combination of Hydrogen (H_2) and Silane (SiH_4) gases. After passivation, on the front surface, 10 nm thick p-type a-Si:H layer was deposited using SiH_4, H_2, and Trimethyl boron (TMB) gases. Similarly, a 10 nm thick n-type a-Si:H layer was deposited on the back surface using SiH_4, H_2, and Phosphine (PH_3) gases. In addition, all cells are deposited with 40 nm of ITO and 220 nm of silver (Ag) on the back surface. In this study, a 100 nm-thick layer of ITO was deposited on front surface (on the p-type a-Si:H layer). Front metallization was achieved using Ag paste via screen-printing. A schematic representation of the SHJ solar cells that was fabricated is shown in Figure 1.

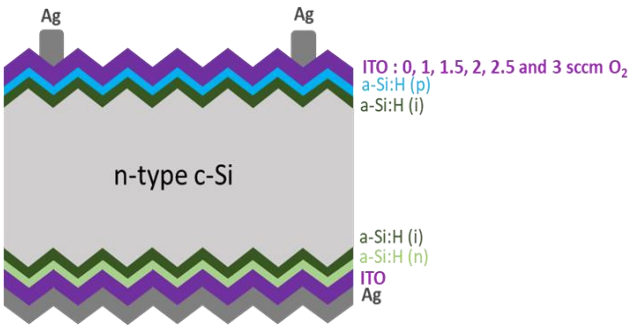

Figure 1. A schematic representation of ITO films deposited on SHJ solar cell

3 Results and discussion

3.1 Structural properties

The structural characteristics of the ITO films were investigated using XRD within a scanning range of 10° to 80° and the XRD patterns were illustrated in Figure 2a. The results indicate that all ITO films exhibited a polycrystalline morphology. The diffraction peaks corresponding to planes (211), (222), (400), (440), and (622) indicate the cubic bixbyite crystal structure. When the amount of oxygen was gradually increased, a decrease in the diffraction peaks corresponding to lattice planes (222), (400), (440), and (622) was observed. There were no detectable diffraction peaks for Sn, SnO or SnO_2, indicating that Sn atoms are incorporated into the In_2O_3 structure. Various crystal structure parameters corresponding to the highest peak, the (222) plane, were calculated for all ITO films deposited at different O_2 ratios and given in Figure 2b and Figure 3. The determination of the crystallite size (D) was performed using the Debye-Scherrer equation Equation (1), which provides a quantitative assessment of this property [19]. The crystallite measurements of the ITO films are presented in Table 2. As shown in Figure 2b an increase in crystallite size corresponds to a decrease in FWHM values. This finding supports that larger crystallite sizes lead to better crystal structures.

$$D = \frac{k\lambda}{\beta cos\theta} \quad (1)$$

The crystallite size tended to decrease with increasing O_2 content. ITO films deposited without O_2 exhibited the largest measured crystallite size at 29 nm, while films deposited with 3 sccm O_2 displayed the smallest size, measuring 15 nm. Specifically, ITO samples deposited using O_2 ratios of 0, 1, and 1.5 sccm displayed an enhanced tendency for crystallization, as indicated by larger crystallite sizes. This observation reiterated the well-established notion that lower oxygen ratios generally create conditions conducive to the development of better-defined and more extensive crystalline domains within films.

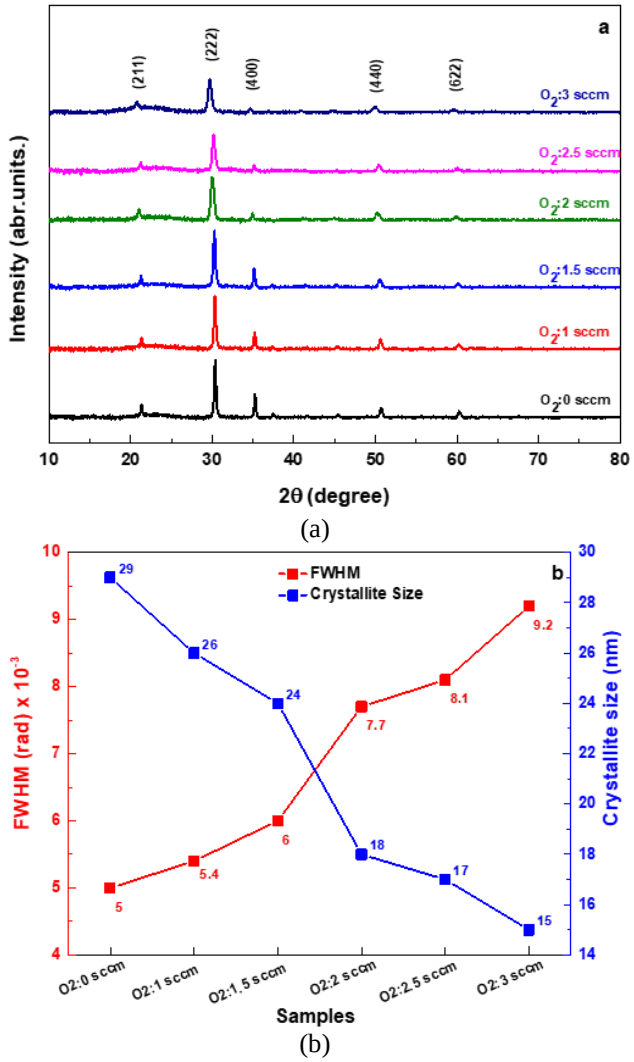

Figure 2. XRD patterns (a) and crystallite size variation versus FWHM (rad) (b) of ITO films deposited on glass substrate at 0, 1, 1.5, 2, 2.5 and 3 sccm O_2 flow rates

Table 2. Parameters used in the calculation of crystallite size (D)

O_2 (sccm)	β (rad) x 10^{-3}	θ (degrees)	cosθ	D (nm)
0	5.0	15.1825	0.9651	29
1	5.4	15.1624	0.9652	26
1.5	6.0	15.1305	0.9653	24
2	7.7	15.0885	0.9655	18
2.5	8.1	15.0108	0.9659	17
3	9.2	14.8560	0.9656	15

Lattice constant (a) for cubic ITO was determined using Equation (2) [20]. The dislocation density (δ) and microstrain (ε) were determined by Equation (3) and (4) [21,22]. Eq. 5 was used to calculate the number of crystallites per unit area (N).

$$\frac{1}{d_{hkl}^2} = \frac{(h^2 + k^2 + l^2)}{a^2} \quad (2)$$

$$\delta = \frac{1}{D^2} \quad (3)$$

$$\varepsilon = \frac{\beta \cot \theta}{4} \quad (4)$$

$$N = \frac{t}{D^3} \quad (5)$$

where t is the film thickness. Important structural characteristics represented by the parameters a, δ, ε, and N associated with ITO films obtained from varying O_2 ratios have been calculated. Figure 3 visually illustrates these parameters, while their numerical representations are given in Table 3. An increase in δ, ε, and N values was observed with increasing O_2 content. This observation confirms that ITO films deposited at O_2 ratios of 0, 1, and 1.5 sccm exhibit better crystal structure and size compared to those deposited at 2, 2.5, and 3 sccm O_2 ratios. The ITO film deposited at 3 sccm O_2 exhibited the highest δ, ε, and N values, while lower values were observed in films deposited at 2.5, 2, 1.5, and 1 sccm O_2, respectively. In contrast, the ITO film obtained at 0 sccm O_2 showed the lowest values among these structural parameters. The increase in dislocation density with higher O_2 content suggests the presence of more crystallographic defects in the films. Such an increase underscores the existence of higher structural irregularities in the crystal lattice [23]. It was seen that the lattice constant values varied in the range of 10.2-10.4 Å according to O_2 ratios and the lattice constant increased with increasing O_2 content.

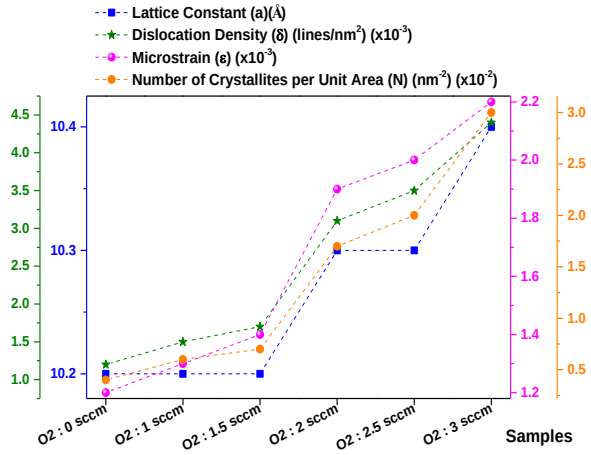

Figure 3. Various structural parameters calculated from XRD data of ITO films deposited at 0, 1, 1.5, 2, 2.5 and 3 sccm O_2 flow rates

Table 3. Various structural values of ITO films deposited at 0, 1, 1.5, 2, 2.5 and 3 sccm O_2 flow rates calculated from XRD data

O_2 (sccm)	LC (a) (Å)	MS (ε) ($x10^{-3}$)	DD (δ) (lines/nm^2) ($x10^{-3}$)	NCA (N) (nm^{-2}) ($x10^{-2}$)
0	10.2	1.2	1.2	0.4
1	10.2	1.3	1.5	0.6
1.5	10.2	1.4	1.7	0.7
2	10.3	1.9	3.1	1.7
2.5	10.3	2.0	3.5	2.0
3	10.4	2.2	4.4	3.0

LC: Lattice Constant **MS:** Microstrain **DD:** Dislocation Density **NCA:** Number of Crystallites per Unit Area

3.2 Optical properties

The transmittance spectra of ITO films at various O_2 flow rates are presented in Figure 4a. The evaluation of transmittance spectra of ITO films reveals a characteristic trend towards increasing transparency in the visible spectral range (400-800 nm). Further analysis reveals that an increase in the O_2 ratio corresponds to an increase in the average transmittance value, but this trend deviates when an O_2 ratio of 3 sccm is reached, after which a decrease in transmittance is recorded. transmittance value, but this trend deviates when an O_2 ratio of 3 sccm is reached, after which a decrease in transmittance is recorded. The peak of the average transmittance is seen in the ITO film deposited at an O_2 rate of 2.5 sccm, recording a transmittance of 80.3%, while the lowest value is captured by the ITO film deposited without O_2, with a transmittance value of 61.0%. The ITO film deposited at O_2 ratios of 2.5 and 3 sccm has the highest transmittance in the near-ultraviolet (UV) spectral region. Remarkably, the increase in O_2 content leads to an increase in transmittance both in the near-UV region and at extended wavelengths. This finding underscores the variations in transmittance trends that can be realized with small adjustments in O_2 flow rates.

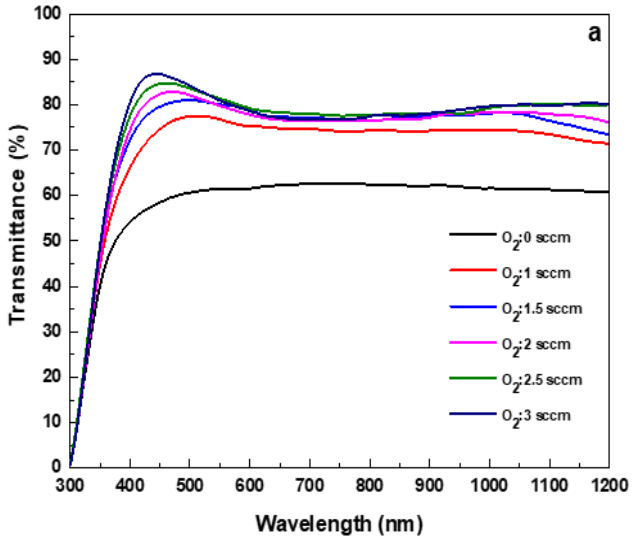

(a)

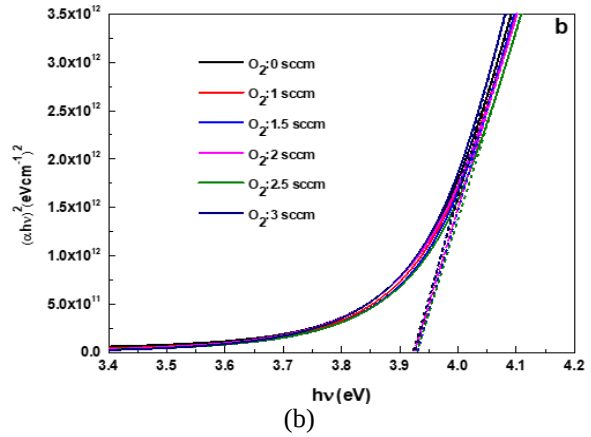

(b)

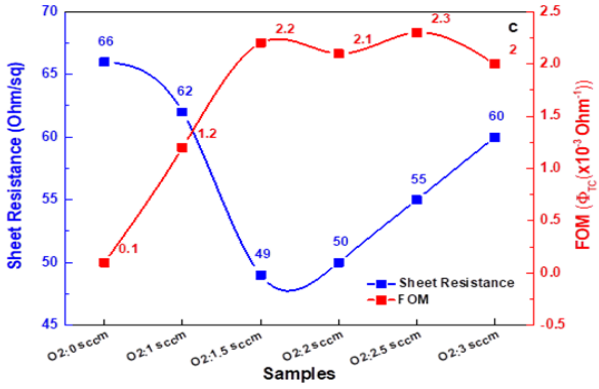

(c)

Figure 4. Transmittance spectra (a), $(\alpha h\nu)^2$ vs photon energy (hν) plot (b) and FOM & R_{sh} results of ITO films deposited at 0, 1, 1.5, 2, 2.5 and 3 sccm O_2 flow rates (c)

The investigation of the optical bandgaps (Eg) of ITO films deposited with different O_2 flow rates has been systematically performed through the analysis of optical transmittance data. The calculation of Eg requires the inclusion of key parameters such as the absorption coefficient (α) and the energy of the photon (hν) [24]. In order to determine the ITO film Eg values, the correlation between $(\alpha h\nu)^2$ and hν is refer to Figure 4b. The Eg values are consistently 3.92 eV across all ITO films under varying O_2 flow rates (Table 4). This tendency emphasizes the consistency in band gap characteristics throughout the range of ITO films. The uniformity of the bandgap values indicates the strength and consistency of ITO films' material properties. The examined O_2 ratios did not significantly affect the bandgap properties.

Table 4. Transmittance and band gap values of ITO films deposited at 0, 1, 1.5, 2, 2.5 and 3 sccm O_2 flow rates

O_2 (sccm)	Average Transmittance(%) (400-800 nm)	Eg (eV)	Transmittance (%) (550 nm)
0	61.0	3.92	61.5
1	74.9	3.92	76.9
1.5	78.3	3.92	79.9
2	78.6	3.92	79.7
2.5	80.3	3.92	81.3
3	80.2	3.92	81.8

3.3 *Electrical properties*

To calculation of the figure of merit (FOM) value of the ITO films, the transmittance values at the 550 nm wavelength are measured (Table 4). The FOM value is calculated via the equation $\phi_{TC} = T^{10}/R_{sh}$, which takes into account both the transmittance and sheet resistance properties of the ITO films at the specific wavelength of 550 nm [25]. Figure 4c represents the calculated ϕ_{TC} values alongside the corresponding sheet resistance (R_{sh}) values of ITO films generated under variable O_2 flow rates. The ϕ_{TC} values increase as the O_2 flow rates increase from 0 sccm to 1.5 sccm. However, the ϕ_{TC} values level-off beyond the 1.5 sccm, as values in this range closely approximate each other. The film deposited at an O_2 ratio of 2.5 sccm has the highest FOM value ($2.3x10^{-3}$ Ohm^{-1}) among all ITO films. As the O_2 flow rate increases from 0 to 1.5 sccm, the sheet resistance value decreases, indicative of an enhanced electrical property. In contrast, this trend leads to a continuous increase in sheet resistance values above the 1.5 sccm threshold, indicating a decrease in electrical property. The film deposited with 0 sccm O_2 flow, exhibited the highest sheet resistance of 66 Ohm/sq. On the other hand, the film deposited with an O_2 ratio of 1.5 sccm displayed the lowest sheet resistance value of 49 Ohm/sq.

The effects of different O_2 flow rates in the deposition of ITO films on the efficiency of SHJ solar cells were also investigated. The important solar cell parameters evaluated are open circuit voltage (V_{OC}), short circuit current (I_{SC}), current density (J_{SC}), voltage at maximum power point (V_{MP}), current at maximum power point (J_{MP}), fill factor (FF), and conversion efficiency (η). Figure 5 shows the solar cell parameters obtained from the SHJ solar cell, while Table 5 gives their corresponding values. It has been observed that the best PV performance is achieved with the average O_2 ratio (2-2.5 sccm) and can be attributed to the reduction of parasitic resistive losses [26-28]. The efficiency of SHJ solar cells shows an initial rise as the O_2 content increases from 0 to 2.5 sccm. However, when the O_2 content reaches 3 sccm, a simultaneous drop in efficiency occurs, reversing the trend seen previously. In particular, the relatively low efficiencies observed in SHJ solar cells fabricated using ITO films with O_2 flow rates of 0 and 1 sccm can be attributed to their low optical properties and high sheet resistance. In the case of SHJ solar cells fabricated from ITO films with O_2 flow rates of 1.5 and 2 sccm, the efficiency levels are relatively low, mainly due to their low optical properties, despite the notable low sheet resistance. For SHJ solar cells fabricated with ITO films characterized by a 3 sccm O_2 flow rate, the higher sheet resistance suppresses the optical properties and results in lower efficiency compared to SHJ solar cells fabricated with ITO films with a 2.5 sccm O_2 flow rate. The result is summarized by the highest efficiency value of 18.6% obtained from SHJ solar cells fabricated using a 2.5 sccm O_2 ratio of ITO. Figure 6 presents the current density-voltage (J-V) plot of SHJ solar cells fabricated in this study.

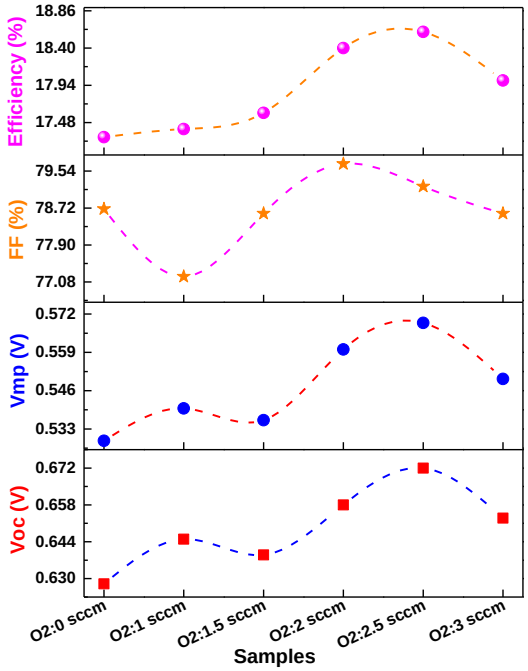

Figure 5. Parameters affecting the SHJ solar cell of ITO films deposited at different O2 ratios (0, 1, 1.5, 2, 2.5 and 3 sccm)

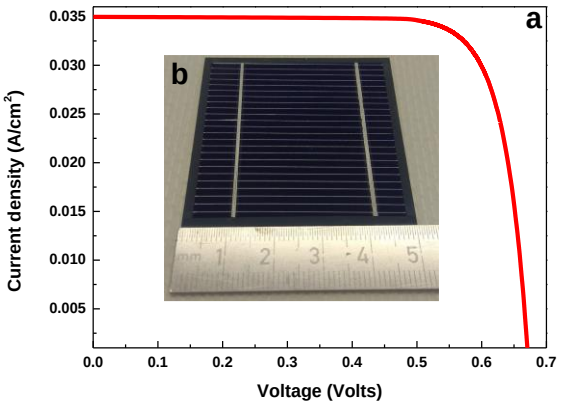

Figure 6. J-V plot of SHJ solar cell deposited at 2.5 sccm O_2 (a) SHJ solar cell deposited in 5x5 cm^2 area (b)

Table 5. SHJ solar cell parameters values of ITO films deposited with different O_2 ratios (0, 1, 1.5, 2, 2.5, and 3 sccm)

Cell (5 x 5 cm^2)	Voc (V)	Isc (A/cm^2)	Jsc (A/cm^2)	Vmp (V)	Jmp (A/cm^2)	FF (%)	Efficiency (η)
O_2:0 sccm	0.628	0.875	0.035	0.529	0.033	78.7	17.3 %
O_2:1 sccm	0.645	0.875	0.035	0.540	0.032	77.2	17.4 %
O_2:1.5 sccm	0.639	0.875	0.035	0.536	0.033	78.6	17.6 %
O_2:2 sccm	0.658	0.875	0.035	0.560	0.033	79.7	18.4 %
O_2:2.5 sccm	0.672	0.875	0.035	0.569	0.033	79.2	18.6 %
O_2:3 sccm	0.653	0.875	0.035	0.550	0.033	78.6	18.0 %

4 Conclusion

The study comprehensively investigates the properties of ITO films on SHJ solar cells. The investigation focused on O_2 ratios (0-3 sccm) during deposition. Optical analysis of visible light (400-800 nm) revealed a strong relationship between O_2 content and film performance. Optimum transmittance (80.3%) occurred at 2.5 sccm O_2, followed by ratios of 3, 2, 1.5, and 1 sccm with decreasing transmittance. The ITO film with 1.5 sccm O_2 showed the lowest sheet resistance (49 Ω/sq) and a FOM value of $2.2x10^{-3}$ Ohm^{-1}. The crystallography was investigated by XRD, confirming well-defined crystallographic planes such as (211), (222), (400), (440), and (622). ITO films with 2.5 sccm O_2 showed promising properties, which achieved an efficiency of 18.6% in SHJ solar cells, demonstrating their importance in advanced optoelectronics due to their structural, optical, and electrical properties.

Acknowledgment

The authors gratefully acknowledge the support from The Scientific and Technological Research Council of Turkey (TÜBİTAK-20AG014).

Conflict of interest

The authors declare no conflict of interest.

Similarity rate (iThenticate): %17

References

[1] T. Damgacı, Küreselleşme Sürecinin Havayolu Ulaştırmasına Etkileri: Küresel Havayolu İş Birlikleri. in: H.A. Kutlu (Ed.), Sosyal, Beşeri ve İdari Bilimler Alanında Gelişmeler 4, Platanus Publishing, pp. 229-252, Ankara, 2023.

[2] J. Khan and M. H. Arsalan, Solar power technologies for sustainable electricity generation–A review. Renewable and Sustainable Energy Reviews, 55, 414-425, 2016. https://doi.org/10.1016/j.rser.2015.10.135

[3] K. O. Ukoba and F. L. Inambao, Study of optoelectronic properties of nanostructured TiO2/NiO heterojunction solar cells. Proceedings of the World Congress on Engineering and Computer Science, 1, 2018. https://doi.org/10.1016/j.conbuildmat.2020.11996

[4] A. Shrestha, G. Mizuno, P. Oduor, R. Olah, S. Islam, A. K. Dutta and N. K. Dhar, High efficiency c-Si solar cells utilizing light-trapping phenomenon. Energy Harvesting and Storage: Materials, Devices, and Applications VI, 9493, pp. 75-81, 2015. https://doi.org/10.1117/12.2183411

[5] A. Yadav, G. Singh, R. Nekovei and R. Jeyakumar, c-Si solar cells formed from spin-on phosphoric acid and boric acid. Renewable Energy, 80, 80-84, 2015. https://doi.org/10.1016/j.renene.2015.01.055

[6] S. Calnan and A. N. Tiwari, High mobility transparent conducting oxides for thin film solar cells. Thin Solid Films, 518(7), 1839-1849, 2010. https://doi.org/10.1016/j.tsf.2009.09.044

[7] A. Varanytsia, L. Weng, T. C. Lin, J. Yang and L. C. Chien, High-performance and low-cost aluminum zinc oxide and gallium zinc oxide electrodes for liquid crystal displays. Journal of Display Technology, 12(10), 1033-1039, 2016. https://doi.org/10.1119/jdt.2016.2584779

[8] A. Ambrosini, A. Duarte, K. R. Poeppelmeier, M. Lane, C. R. Kannewurf and T. O. Mason, Electrical, optical, and structural properties of tin-doped In2O3–M2O3 solid solutions (M= Y, Sc). Journal of Solid State Chemistry, 153(1), 41-47, 2000. https://doi.org/10.1006/jssc.2000.8737

[9] J. M. Gaskell and D. W. Sheel, Deposition of indium tin oxide by atmospheric pressure chemical vapour deposition. Thin Solid Films, 520(12), 4110-4113, 2012. https://doi.org/10.1016/j.tsf.2011.04.191

[10] M. J. Alam and D. C. Cameron, Optical and electrical properties of transparent conductive ITO thin films deposited by sol–gel process. Thin Solid Films, 377, 455-459, 2000. https://doi.org/10.1016/S0040-6090(00)01369-9

[11] H. N. Cui, V. Teixeira, L. J. Meng, R. Martins and E. Fortunato, Influence of oxygen/argon pressure ratio on the morphology, optical and electrical properties of ITO thin films deposited at room temperature. Vacuum, 82(12), 1507-1511, 2008. https://doi.org/10.1016/j.vacuum.2008.03.061

[12] A. Iljinas, I. Mockevičius, M. Andrulevičius, Š. Meškinis and S. Tamulevičius, Growth of ITO thin films by magnetron sputtering: OES study, optical and electrical properties. Vacuum, 83, S118-S120, 2009. https://doi.org/10.1016/j.vacuum.2009.01.040

[13] S. Q. Hussain, S. Kim, S. Ahn, N. Balaji, Y. Lee, J. H. Lee and J. Yi, Influence of high work function ITO: Zr films for the barrier height modification in a-Si: H/c-Si heterojunction solar cells. Solar Energy Materials and Solar Cells, 122, 130-135, 2014. https://doi.org/10.1016/j.solmat.2013.11.031

[14] Y. Demirhan, H. Koseoglu, F. Turkoglu, Z. Uyanik, M. Ozdemir, G. Aygun and L. Ozyuzer, The controllable deposition of large area roll-to-roll sputtered ito thin films for photovoltaic applications. Renewable Energy, 146, 1549-1559, 2020. https://doi.org/10.1016/j.renene.2019.07.038

[15] S. Boycheva, A. K. Sytchkova, M. L. Grilli and A. Piegari, Structural, optical and electrical peculiarities of rf plasma sputtered indium tin oxide films. Thin Solid Films, 515(24), 8469-8473, 2007. https://doi.org/10.1016/j.tsf.2007.03.165

[16] M. Shakiba, A. Kosarian and E. Farshidi, Effects of processing parameters on crystalline structure and optoelectronic behavior of DC sputtered ITO thin film. Journal of Materials Science: Materials in Electronics, 28, 787-797, 2017. https://doi.org/10.1007/s10854-016-5591-1

[17] A. Seyhan and E. Kartal, Optical, Electrical and Structural Properties of ITO/IZO and IZO/ITO Multilayer Transparent Conductive Oxide Films

Deposited via Radio frequency Magnetron Sputtering. Coatings, 13(10), 1719, 2023. https://doi.org/10.3390/coatings13101719

[18] E. Kartal, İ. Duran, E. Damgaci and A. Seyhan, Investigation of Structural, Optical, and Electrical Properties of ITO Films Deposited at Different Plasma Powers: Enhanced Performance and Efficiency in SHJ Solar Cells. Eurasian Journal of Science Engineering and Technology, 4(1), 25-35, 2023. https://doi.org/10.55696/ejset.1297942

[19] S. Parthiban, E. Elangovan, K. Ramamurthi, D. Kanjilal, K. Asokan, R. Martins and E. Fortunato, Effect of Li3+ heavy ion irradiation on the Mo doped In2O3 thin films prepared by spray pyrolysis technique. Journal of Physics D: Applied Physics, 44(8), 085404, 2011. https://doi.org/10.1088/0022-3727/44/8/085404

[20] M. N. Rezaie, N. Manavizadeh, F. D. Nayeri, M. M. Bidgoli, E. Nadimi and F. A. Boroumand, Effect of seed layers on low-temperature, chemical bath deposited ZnO nanorods-based near UV-OLED performance. Ceramics International, 44(5), 4937-4945, 2018. https://doi.org/10.1016/j.ceramint.2017.12.086

[21] M. Thirumoorthi and J. T. J. Prakash, Structural, morphological characteristics and optical properties of Y doped ZnO thin films by sol–gel spin coating method. Superlattices and Microstructures, 85, 237-247, 2015. https://doi.org/10.1016/j.spmi.2015.05.005

[22] K. Mageshwari and R. Sathyamoorthy, Physical properties of nanocrystalline CuO thin films prepared by the SILAR method. Materials Science in Semiconductor Processing, 16(2), 337-343, 2013. https://doi.org/10.1016/j.mssp.2012.09.016

[23] P. Sarker, S. K. Sen, M. N. H. Mia, M. F. Pervez, A. A. Mortuza, S. Hossain and M. A. M. Chowdhury, Effect of gamma irradiation on structural, morphological and optical properties of thermal spray pyrolysis deposited CuO thin film. Ceramics International, 47(3), 3626-3633, 2021. https://doi.org/10.1016/j.ceramint.2020.09.211

[24] K. Zhang, F. Zhu, C. H. A. Huan and A. T. S. Wee, Indium tin oxide films prepared by radio frequency magnetron sputtering method at a low processing temperature. Thin Solid Films, 376(1-2), 255-263, 2000. https://doi.org/10.1016/S0040-6090(00)01418-8

[25] K. Kacha, F. Djeffal, H. Ferhati, L. Foughali, A. Bendjerad, A. Benhaya and A. Saidi, Efficiency improvement of CIGS solar cells using RF sputtered TCO/Ag/TCO thin-film as prospective buffer layer. Ceramics International, 20194-20200, 2022. https://doi.org/10.1016/j.ceramint.2022.03.298

[26] B. Aïssa, Y. Zakaria, A. A. Abdallah, M. M. Kivambe, A. Samara, A. R. Shetty and C. Ballif, Impact of the Oxygen Flow during the Magnetron Sputtering Deposition on the Indium Tin Oxide thin films for Silicon Heterojunction Solar Cell. In 2019 IEEE 46th Photovoltaic Specialists Conference (PVSC), pp. 2659-2666, IEEE, 2019. https://doi.org/10.1109/PVSC40753.2019.8980906

[27] W. Gong, G. Wang, Y. Gong, L. Zhao, L. Mo, H. Diao and W. Wang, Investigation of In2O3: SnO2 films with different doping ratio and application as transparent conducting electrode in silicon heterojunction solar cell. Solar Energy Materials and Solar Cells, 111404, 2022. https://doi.org/10.1016/j.solmat.2021.111404

[28] A. Chen and K. Zhu, Effects of TCO work function on the performance of TCO/n-Si hetero-junction solar cells. Solar Energy, 195-201, 2014. https://doi.org/10.1016/j.solener.2014.06.005